Solution Method for Nonlinear Problems with Multiple Critical Points

Yeong-Bin Yang* and Ming-Shan Shieh†
National Taiwan University, Taipei, Taiwan, Republic of China

An improved method is presented for solving nonlinear problems with multiple limit points and snap-back points. It is formulated in $N + 1$ dimensional space that includes one load parameter and N displacements as the unknowns. To solve these unknowns, a constraint equation is needed in addition to the N equations of equilibrium. Whether the constraint equation is proper can be justified from the bounded nature of the load parameter. The method presented herein may be referred to as the "generalized displacement control method." With the introduction of a general stiffness parameter, the method has been demonstrated to be numerically stable at the critical points, effective in adjusting the step sizes, and self-adaptive in changing the loading directions. Two examples with curves of the looping type have been solved by the present method for illustration.

Introduction

THE basic problem in a geometrically nonlinear analysis is the solution of a set of nonlinear equations for the structure. Depending on the history of loading, the stiffness of the structure may be softening or stiffening, the equilibrium path may be stable or unstable, and the structure itself may be on a stage of loading or unloading. All such phenomena are typified by the occurrence of critical points such as the limit points and snap-back points in the load-deflection curves (Fig. 1).

The solution of nonlinear problems is usually attempted by a combination of the incremental and iterative schemes. A requirement for the nonlinear solution method is its ability to overcome the numerical problems associated with each type of behaviors. Three criteria can be stated here. First, the method should be self-adaptive in changing the loading direction at the limit points. Second, numerical stability for iterations should be maintained at all regions, including those near the critical points. Finally, adjustment in step sizes should be made automatically to reflect the stiffening and softening of the structure.

Mathematically speaking, in a nonlinear analysis, one is faced with the problem of solving the $N + 1$ system equations (i.e., N equations of equilibrium and one constraint equation) for the $N + 1$ system parameters (i.e., N displacements and one load parameter). To this end, the following methods have been used: the Newton-Raphson method, the displacement control method,[1-3] the arc length method,[4-9] and the work control method,[10,11] among others. Each of these methods differs in the use of different constraint equations for the incremental and iterative steps.[11] In terms of the criteria set previously, none of these methods is perfect for nonlinear problems with multiple occurrence of critical points.

A new formulation based fully on $N + 1$ dimensional space will be presented in this paper. Such a formulation allows one to evaluate algebraically whether a constraint equation is appropriate for general nonlinear analysis, based on the bounded nature of the load increment parameter for the iterative steps. Through the introduction of a general stiffness parameter, a solution method that is believed to be superior to most of the existing methods is proposed.

Received July 31, 1989; revision received Jan. 18, 1990.

*Professor, Department of Civil Engineering.
†Graduate Student, Department of Civil Engineering.

Statement of Problem

In the present study, the notation [ ] will be used for a square matrix, { } for a column vector, and < > for a row vector. The matrix equation for the jth iteration of the ith increment of a nonlinear system with N degrees of freedom can be written as

$$[K]^i_{j-1}\{u\}^i_j = \lambda^i_j\{P\} + \{R\}^i_{j-1} \tag{1}$$

where $[K]$ is the tangent stiffness matrix of the structure, $\{u\}$ the displacement increment vector, $\{P\}$ the reference load vector, λ the load increment parameter, and $\{R\}$ the unbalanced force vector. In general, both $\{u\}$ and λ are assumed to be unknown. To solve this problem, a constraint equation is required in addition to the preceding N equations. The following is a general form of the constraint equation:

$$<C>\{u\}^i_j + k\lambda^i_j = H^i_j \tag{2}$$

The reliability and efficiency of a nonlinear solution scheme hinges on the selection of the constants $\{C\}$ and k and the parameter H^i_j for the constraint equation, as will be demonstrated later on.

According to Batoz and Dhatt,[12] Eq. (1) can be conveniently replaced by the following equations:

$$[K]^i_{j-1}\{u_1\}^i_j = \{P\} \tag{3a}$$

$$[K]^i_{j-1}\{u_2\}^i_j = \{R\}^i_{j-1} \tag{3b}$$

$$\{u\}^i_j = \lambda^i_j\{u_1\}^i_j + \{u_2\}^i_j \tag{4}$$

where the load increment parameter λ^i_j is to be determined from the constraint equation, Eq. (2).

Theory in $N + 1$ Dimensional Space

The preceding governing equations and constraint equation, Eqs. (2-4), can be combined into a single matrix equation in $N + 1$ dimensional space as follows:

$$[\bar{K}_1]^i_{j-1}\begin{Bmatrix}\lambda^i_j\{u_1\}^i_j\\ \lambda^i_j\end{Bmatrix} + [\bar{K}_2]^i_{j-1}\begin{Bmatrix}\{u_2\}^i_j\\ 1\end{Bmatrix} = \begin{Bmatrix}\{0\}\\ H^i_j\end{Bmatrix} \tag{5}$$

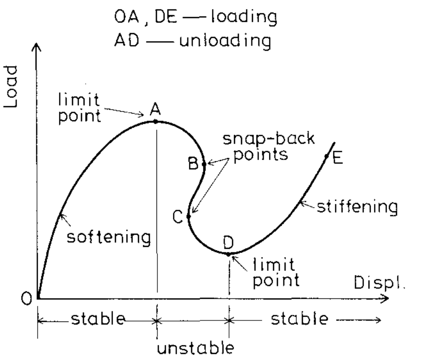

Fig. 1 General characteristics of a nonlinear system.

where the generalized stiffness matrices $[\bar{K}_1]$ and $[\bar{K}_2]$ in $N + 1$ dimensional space are defined as

$$[\bar{K}_1]^i_{j-1} = \begin{bmatrix} [K]^i_{j-1} & -\{P\} \\ <C> & k \end{bmatrix} \tag{6a}$$

$$[\bar{K}_2]^i_{j-1} = \begin{bmatrix} [K]^i_{j-1} & -\{R\}^i_j \\ <C> & 0 \end{bmatrix} \tag{6b}$$

The $N \times N$ stiffness matrix $[K]$ can be decomposed using the triple-factoring method as follows[13]:

$$[K] = [L][D][L]^T \tag{7}$$

where $[D]$ is the diagonal matrix and $[L]$ the lower triangular matrix with all of its diagonal elements declared to be unity. Accordingly, the determinant of $[K]$ is equal to that of $[D]$,

$$\det[K] = \det[D] \tag{8}$$

By adopting the following definitions for $\{T_1\}$ and $\{T_2\}$

$$-\{P\} = [L][D]\{T_1\} \tag{9a}$$

$$\{C\} = [L][D]\{T_2\} \tag{9b}$$

the generalized stiffness matrix $[\bar{K}_1]$ can be decomposed as follows:

$$[\bar{K}_1] = \begin{bmatrix} [L] & 0 \\ <T_2> & 1 \end{bmatrix} \begin{bmatrix} [D] & 0 \\ 0 & d \end{bmatrix} \begin{bmatrix} [L] & \{T_1\} \\ 0 & 1 \end{bmatrix} \tag{10}$$

where

$$d = k - <T_2>[D]\{T_1\} \tag{11}$$

Consequently, the determinant of the generalized stiffness matrix $[\bar{K}]$ becomes

$$\det[\bar{K}_1] = (k - <T_2>[D]\{T_1\}) \det[K] \tag{12}$$

Making use of Eqs. (9), one obtains

$$<T_2>[D]\{T_1\} = -<C>[K]^{-1}\{P\} \tag{13}$$

Substituting Eq. (13) into Eq. (12) yields

$$\det[\bar{K}_1] = (k + <C>[K]^{-1}\{P\}) \det[K] \tag{14}$$

or

$$\det[\bar{K}_1] = (k + <C>\{u_1\}) \det[K] \tag{15}$$

through use of Eq. (3a).

Rearranging Eq. (5) yields the following form:

$$\begin{Bmatrix} \lambda^i_j \{u_1\}^i_j \\ \lambda^i_j \end{Bmatrix} = ([\bar{K}_1]^{-1})^i_{j-1} \begin{Bmatrix} \{0\} \\ H^i_j \end{Bmatrix} - ([\bar{K}_1]^{-1})^i_{j-1} [\bar{K}_2]^i_{j-1} \begin{Bmatrix} \{u_2\}^i_j \\ 1 \end{Bmatrix} \tag{16}$$

This equation clearly indicates that, for the system parameters λ^i_j and $\{u_1\}^i_j$ to be bounded, the determinant of the generalized stiffness $[\bar{K}_1]$, rather than the tangent stiffness $[K]$, must be nonzero. The inverse matrix $[\bar{K}_1]^{-1}$ can be represented by

$$[\bar{K}_1]^{-1} = \frac{1}{\det[\bar{K}_1]} \begin{bmatrix} [A] & \{D_1\} \\ <D_2> & \det[K] \end{bmatrix} \tag{17}$$

where $[A]$, $\{D_1\}$, and $\{D_2\}$ are matrix and vectors consisting of cofactors of the elements in $[\bar{K}_1]$. Using Eqs. (17) and (6b), one obtains

$$[\bar{K}_1]^{-1}[\bar{K}_2] = \frac{1}{\det[\bar{K}_1]} \times \begin{bmatrix} [A][K] + \{D_1\}<C> & -[A]\{R\} \\ <D_2>[K] + \det[K]<C> & -<D_2>\{R\} \end{bmatrix} \tag{18}$$

Substitution of Eqs. (17) and (18) into the last row of Eq. (16) along with the use of Eqs. (3b) and (15) yields

$$\lambda^i_j = \frac{1}{<C>\{u_1\}^i_j + k} (H^i_j - <C>\{u_2\}^i_j) \tag{19}$$

Equation (19) serves as a useful basis for evaluating the numerical stability of the nonlinear solution methods. A solution method is said to be numerically stable only when both the load and displacement increments λ^i_j and $\{u\}^i_j$ [Eq. (4)] remain bounded through the entire history of loading. Whenever the load or displacement increments cease to be bounded at certain points, numerical instability or divergence will occur at such points in the load-deflection analysis.

Comments on Existing Solution Methods

Based on the criteria just described, some of the commonly used solution methods will be evaluated in this section. It should be noted that the same criteria can be used to evaluate other methods existing in the literature as the constraint equations are concerned.

Newton-Raphson Method

The original Newton-Raphson method performs iteration at constant load. This is equivalent to the use of $\{C\} = \{0\}$, $k = 1$, H^i_1 is a prescribed load increment, and $H^i_j = 0$ for $j \geq 2$. Substituting these parameters into Eq. (19) yields

$$\lambda^i_j = \begin{cases} \text{prescribed load increment} & \text{for } j = 1 \\ 0 & \text{for } j \geq 2 \end{cases} \tag{20}$$

where it should be noted that $\{R\}^i_1 = \{u_2\}^i_1 = \{0\}$ for the incremental step ($j = 1$). Although the load increment λ^i_j remains to be bounded, actually equal to zero, for iterative steps with $j \geq 2$, one should not forget that, as the limit point is approached, the determinant of the stiffness matrix $[K]$ will approach zero. There exists the possibility for the displacement increment $\{u\}^i_j (= \{u_2\}^i_j)$ to approach infinity [see Eqs. (3) and (4)]. Evidently, numerical instability may occur near the limit points.

Displacement Control Method

Let the cth component of displacements be the control displacement. The following are assumed: $<C> = <\mathbf{0} \dots \mathbf{0}\ \mathbf{1}\ \mathbf{0} \dots \mathbf{0}>$, where all elements are zero except the cth; $k = 0$; H^i_1 is a prescribed displacement increment; and $H^i_j = 0$ for $j \geq 2$.

Substituting these parameters into Eq. (19) yields

$$\lambda_j^i = \begin{cases} H_1^i / u_{11}^c & \text{for } j = 1 \\ -u_{2j}^c / u_{1j}^c & \text{for } j \geq 2 \end{cases} \tag{21}$$

Obviously, both the load increment λ_j^i [see Eq. (21)] and the displacement increments $\{u\}_j^i$ [see Eq. (4)] are of finite magnitudes in the vicinity of limit points. This confirms the capability of the displacement control method in dealing with the limit points. Now, suppose that the control displacement u^c snaps back at loading stages. As the snap-back point is approached, the control displacement u_1^c will approach zero. From Eq. (21), one observes that the load increment λ_j^i will approach infinity in accordance. Therefore, numerical instability will occur at these points.

Arc Length Method

Previously, various iterative vectors have been used by researchers in applying the arc length procedures. For the present purposes, only the arc length method with fixed normal plane in $N + 1$ dimensional space will be discussed. By assuming the following for the incremental step ($j = 1$): $\{C\} = \{u\}_1^i$ $(= \lambda_1^i \{u_1\}_1^i)$, $k = \lambda_1^i$, and $H_1^i = \Delta S^2$, where ΔS is a prescribed arc length, the load increment parameter can be solved from Eq. (19):

$$\lambda_1^i = \pm \left(\frac{\Delta S^2}{1 + \langle u_1 \rangle_1^i \{u_1\}_1^i} \right)^{1/2} \tag{22}$$

By setting ΔS to zero, the load increment parameter can be obtained from Eq. (19) for the iterative steps as follows:

$$\lambda_j^i = -\frac{\langle u \rangle_1^i \{u_2\}_j^i}{\langle u \rangle_1^i \{u_1\}_j^i + \lambda_1^i} \qquad \text{for } j \geq 2 \tag{23}$$

Because of the different unit used by each quantity in Eq. (23), the possibility exists for the parameter k $(= \lambda_1^i)$ to be so large that the sign of λ_j^i depends fully on the angle between $\{u\}_1^i$ and $\{u_2\}_j^i$. It follows that, in the vicinity of snap-back points with sharp gradients, an improper sign may be obtained for the load parameter λ_j^i, which eventually may lead to incorrect iterative directions and numerical divergence. Another drawback with the arc length method in its present form is the lack of information for determining the change in loading directions, i.e., the + and − signs in Eq. (22).

Work Control Method

Let $\{C\} = \lambda_j^i \{P\}$, $k = 0$, $H_1^i = \Delta W$ (a prescribed work increment), and $H_j^i = 0$ for $j \geq 2$. Substitution of these parameters in Eq. (19) yields

$$\lambda_1^i = \pm \left(\frac{\Delta W}{\langle P \rangle \{u_1\}_1^i} \right)^{1/2} \tag{24}$$

for the incremental step, and

$$\lambda_j^i = -\frac{\langle P \rangle \{u_2\}_j^i}{\langle P \rangle \{u_1\}_j^i} \qquad \text{with } j \geq 2 \tag{25}$$

for the iterative steps. By defining the current stiffness parameter (CSP) as[14]

$$\text{CSP} = \frac{\langle P \rangle \{u_1\}_1^1}{\langle P \rangle \{u_1\}_1^i} \tag{26}$$

Eq. (24) can be rewritten as[11]

$$\lambda_1^i = \lambda_1^1 \, (\text{CSP})^{1/2} \tag{27}$$

where λ_1^i and λ_1^1 are the load increments at the current and first load steps, respectively. This method generally is good for tracing paths with limit points, but only with limited success for snap-back points. For instance, for structures with a small number of degrees of freedom, the terms $\langle P \rangle \{u_1\}_j^i$ may approach zero as the displacement associated with the major loading direction tends to snap back. As a result, the CSP of Eq. (26) will also approach infinity, thereby resulting in numerical divergence. This is certainly a drawback of the CSP, as will be discussed later on. One weak point with the work control method is the use of the $\{P\}$ vector as the weighting parameter in Eq. (25). This vector, being arbitrary in nature, is not a good representation of the structural properties.

Proposed Method of Solution

It has been demonstrated that most of the existing methods are not perfect in terms of the following criteria: 1) numerical stability in approaching the limit points and snap-back points, 2) adjustable load increments to reflect the variation in stiffness, and 3) self-adaptive capability in determining the loading direction. In addition, it has been shown that numerical stability of a solution method hinges on the bounded characteristics of the load increment parameter λ_j^i, which, in turn, relies on the selection of proper constants $\{C\}$, k, and H_j^i for the constraint, as can be seen from Eq. (19).

Based on the preceding considerations, the following are adopted in the present study: $k = 0$ and $\{C\} = \lambda_1^i \{u_2\}_1^{i-1}$. From Eq. (19), one obtains

$$\lambda_j^i = \frac{H_j^i - \lambda_1^i \langle u_1 \rangle_1^{i-1} \{u_2\}_j^i}{\lambda_1^i \langle u_1 \rangle_1^{i-1} \{u_1\}_j^i} \tag{28}$$

where $\{u_1\}_1^{i-1}$ is the displacement resulting from the first iteration of the last incremental step and H_j^i should be interpreted as a generalized displacement. Since $\{u_2\}_j^i = \{\mathbf{0}\}$ for $j = 1$ and $H_j^i = 0$ for $j \geq 2$, one obtains from Eq. (28)

$$\lambda_1^i = \left(\frac{H_1^i}{\langle u_1 \rangle_1^{i-1} \{u_1\}_1^i} \right)^{1/2} \tag{29}$$

for the incremental step, and

$$\lambda_j^i = -\frac{\langle u_1 \rangle_1^{i-1} \{u_2\}_j^i}{\langle u_1 \rangle_1^{i-1} \{u_1\}_j^i} \qquad \text{with } j \geq 2 \tag{30}$$

for the iterative steps. For $i = 1$, $\{u_1\}_1^0$ will be taken equal to $\{u_1\}_1^1$. From Eq. (29), one obtains

$$H_1^i = (\lambda_1^1)^2 \langle u_1 \rangle_1^1 \{u_1\}_1^1 \tag{31}$$

which may be substituted back into Eq. (29) to yield

$$\lambda_1^i = \lambda_1^1 \left(\frac{\langle u_1 \rangle_1^1 \{u_1\}_1^1}{\langle u_1 \rangle_1^{i-1} \{u_1\}_1^i} \right)^{1/2} \tag{32}$$

Further, by introducing a generalized stiffness parameter

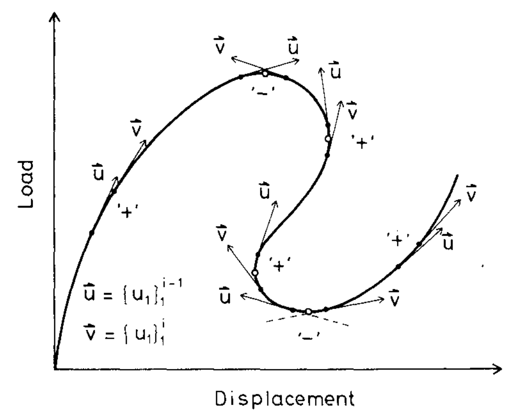

Fig. 2 Characteristics of GSP.

(GSP) as follows

$$\mathrm{GSP} = \frac{\langle u_1 \rangle_1^1 \{u_1\}_1^1}{\langle u_1 \rangle_1^{i-1} \{u_1\}_1^i} \tag{33}$$

the load increment parameter λ_1^i for the ith step can be computed as

$$\lambda_1^i = \lambda_1^1 \, (\mathrm{GSP})^{1/2} \tag{34}$$

with the load increment λ_1^1 prescribed for the first load step.

The method of solution present herein may be referred to as the generalized displacement control method. It is superior to most of the existing methods for the following reasons: First, numerical stability can always be achieved in regions near the limit points and snap-back points, i.e., both the load parameter λ_j^i and $\{u\}_j^i$ will remain bounded in these regions. Second, variation in nonlinearity of the structure has been taken into account through inclusion of the GSP in the load parameter of Eq. (34). Finally, a sign change in the GSP at the limit points serves as a good indicator for reversing the loading direction. A close look at the properties of GSP should help clarify the earlier points of view. This will be elaborated in the following section.

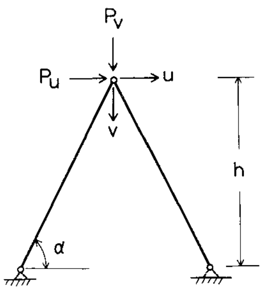

Fig. 3 Two-member truss.

General Stiffness Parameter vs Current Stiffness Parameter

The CSP, as proposed by Bergan,[14] often has been used to monitor the stiffness of a structure in nonlinear analyses.[11,15] Starting with an initial value of unity, it becomes greater than unity when the structure gets stiffer, and vice versa. A zero value for the CSP implies the occurrence of a limit point. Despite these useful characteristics, the CSP is not suitable for solving nonlinear problems with multiple critical points.

First of all, the CSP changes sign at both limit points and snap-back points, as will be seen later. This has rendered the CSP an inadequate indicator for reversing the loading direction if one realizes that change in loading directions should be made only at the limit points. Moreover, the CSP varies in an abrupt manner in the vicinity of snap-back points. Numerical difficulties will occur due to the lack of smoothness in the CSP, if one tries to link the load step size to the CSP, say, using formulas such as the one in Eq. (27) for the work control method.

The GSP, as defined in Eq. (33), has several important characteristics:

1) The numerator and denominator in Eq. (33) represent the

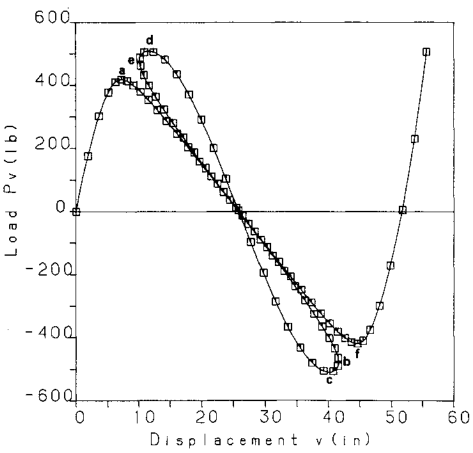

a) Load P_v vs displacement v

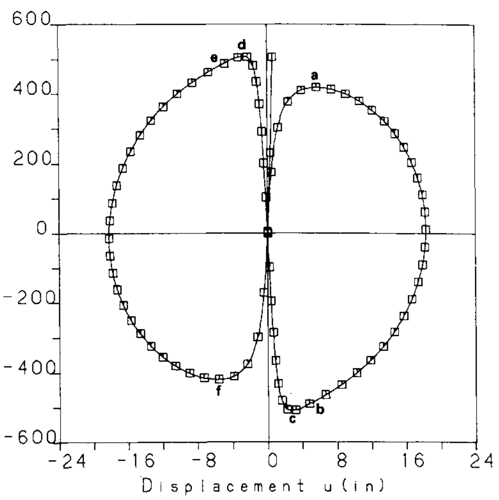

b) Load P_v vs displacement u

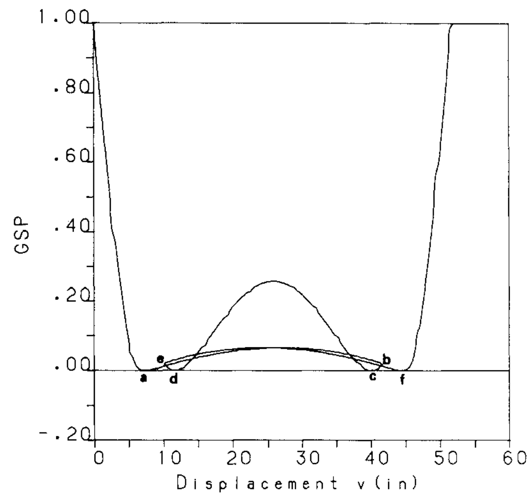

c) GSP vs displacement v

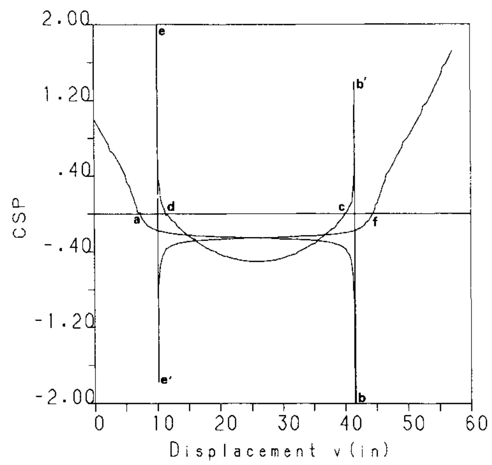

d) CSP vs displacement v

Fig. 4 Load case 1 for two-member truss (1 in. = 2.54 cm; 1 lb = 4.45 N).

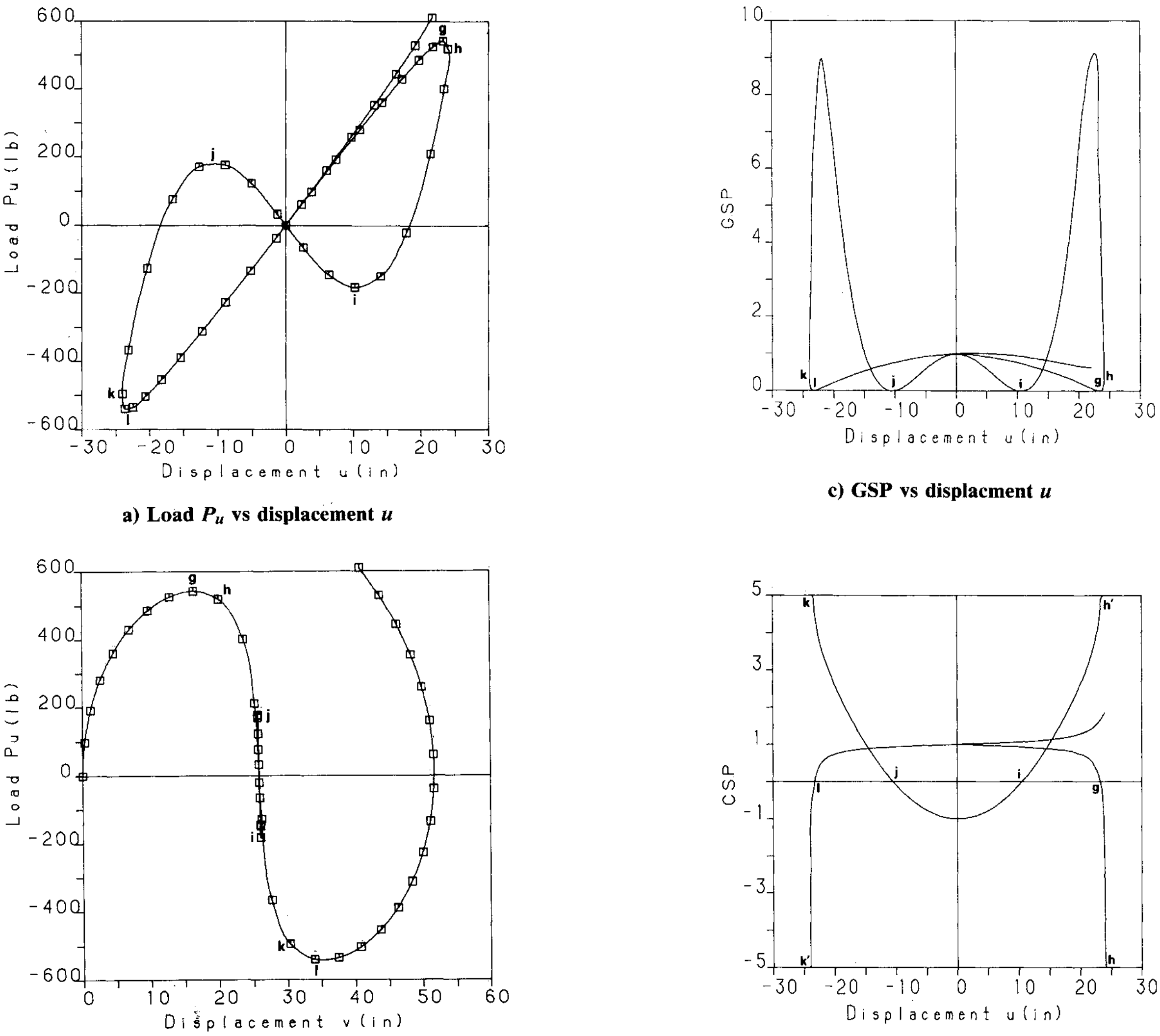

a) Load P_u vs displacement u

b) Load P_u vs displacement v

c) GSP vs displacment u

d) CSP vs displacement u

Fig. 5 Load case 2 for two-member truss (1 in. = 2.54 cm; 1 lb = 4.45 N).

displacements at the first step and approximately those at the current step. Thus, the GSP is representative of the stiffness of the structure at the current step. Further, it has the advantage that no jump in numerical value may occur even in regions near the snap-back points.

2) The GSP is negative only for the load steps "immediately after" the limit points, whereas for the other load steps, it will always be positive. This can be attributed to the fact that the sign of GSP depends fully on the two vectors $\{u_1\}_1^{i-1}$ and $\{u_2\}_1^i$, as can be seen from Eq. (33) and Fig. 2. The GSP by itself is a useful indicator for changing the loading directions.

3) The GSP, as well as the CSP, starts with unity and is zero at the limit points.

Algorithm for the Present Method

The method proposed herein can be incorporated easily in a general purpose program for solving geometrically nonlinear problems. Following is a brief procedure for applying the method:

1) Select a basic load increment λ_1^1 for starting.

2) For the first iteration ($j = 1$) in any step i:

a) Form the structural stiffness matrix $[K]_0^i$.

b) Solve the equations of equilibrium, Eq. (3a), for $\{u_1\}_1^i$. For $i = 1$, let GSP = 1. For $i \geq 2$, use Eq. (33) to determine GSP.

c) For $i \geq 2$, use Eq. (34) to determine λ_1^i.

d) Check if GSP is negative. If yes, multiply λ_1^i by -1 to reverse the loading direction.

e) Determine the displacement using Eq. (4), noting that $\{u_2\}_1^i = \{0\}$.

3) For subsequent iterations ($j \geq 2$):

a) Determine the out-of-balanced forces $\{R\}_{j-1}^i$.

b) Update the stiffness matrix $[K]_{j-1}^i$ (optional).

c) Solve Eqs. (3a) and (3b) for the displacements $\{u_1\}_j^i$ and $\{u_2\}_j^i$.

d) Use Eq. (30) to determine the load increment λ_j^i.

e) Compute the displacements $\{u\}_j^i$ for the current iteration using Eq. (4).

4) Update the element forces, load level, and geometry.

5) Repeat steps 3) and 4) until the desired accuracy is obtained.

6) If the total load does not exceed the maximum load allowed, return to step 2) for the next increment. Otherwise, stop the procedure.

Numerical Examples

This section has the objective of numerically evaluating the applicability and reliability of the method of solution presented in this paper.

Example 1

The two-member truss shown in Fig. 3 has been widely used as a benchmark problem for comparison of numerical solu-

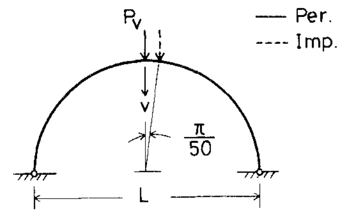

Fig. 6 Hinged circular arch.

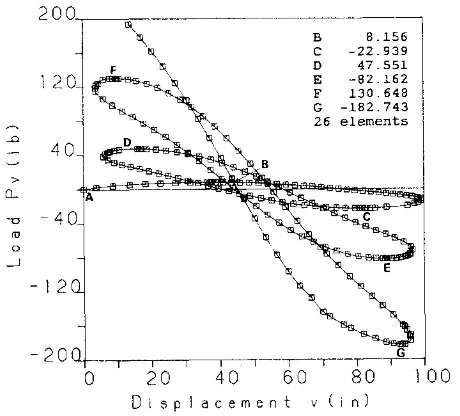

Fig. 7 Deformation curve for arch under symmetric loading (1 in. = 2.54 cm; 1 lb = 4.45 N).

tion algorithms.[16] The following are assumed: axial rigidity $EA = 1884.694$ lb (8366.888 N), $h = 25.847$ in. (65.651 cm), and $\alpha = 63.4$ deg. Two loading cases will be studied herein. In the first case, the horizontal load is considered as an imperfection, i.e., $P_u = 0.05P_v$. The results obtained by the present method are shown in Figs. 4a and 4b, which are in good agreement with the exact solutions of Ref. 16. As can be seen from Fig. 4a, there are four limit points a, c, d, and f, and two snap-back points b and e. The present analysis has demonstrated the self-adaptive capability of the proposed method in coping with the critical points, in adjusting the load step sizes, and in reversing the loading directions. The control parameter GSP, as shown in Fig. 4c, represents a significant improvement over the CSP of Fig. 4d, in that the discontinuity at the snap-back points has been removed.

In the second case, the vertical load is treated as an imperfection, i.e., $P_v = 0.05P_u$. The load-deflection curves are drawn in Figs. 5a and 5b, whereas the GSP and CSP curves are shown in Figs. 5c and 5d, respectively. The observations made for the first load case can also be applied here.

Example 2

The hinged circular arch shown in Fig. 6 has been studied previously by Harrison.[17] The following data were used: $L = 100$ in. (254 cm), modulus of elasticity $E = 200$ psi (1378 kPa), moment of inertia $I = 1$ in.^{4} (41.62 cm^4), and sectional area $A = 10$ in.^{2} (64.52 cm^2). In the present study, the arch was represented by 25 straight elements of equal length. In particular, the central element was further divided into two elements so that the load can be applied at the central point. Two loading cases are considered. One is the case with the load applied symmetrically at the central point; the other assumes the load to be displaced a small distance to the next nodal point (see Fig. 6) so as to produce the effect of imperfection. The finite element adopted hereing is a two-dimensional straight beam with three degrees of freedom, i.e., two translations and one rotation, at each of the two ends. In calculating the element forces, the effects of rigid-body motions on existing nodal forces are considered, whereas the incremental element forces are calculated through the concept of member (or natural) deformations. Detailed description of the element

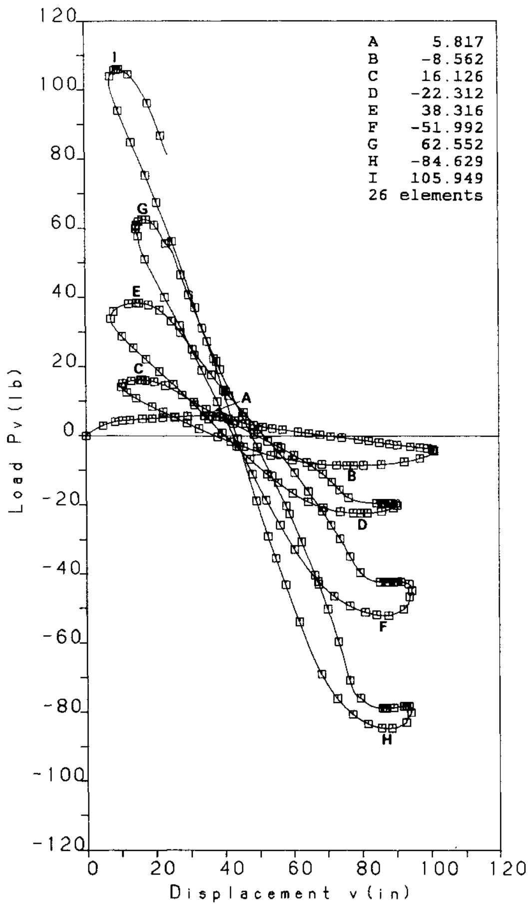

Fig. 8 Deformation curve for arch under asymmetric loading (1 in. = 2.54 cm; 1 lb = 4.45 N).

properties and the associated force recovery procedure can be found in Ref. 18. Figures 7 and 8 show the load-deflection curves for the circular arch under symmetric and asymmetric loadings, respectively. Note that for extremely large deformation problems such as the present one, a great number of elements should be used to ensure the accuracy of solution. Though only 26 elements were used herein, the solutions obtained appear to be close in trend to those of Ref. 17, which used a finer mesh of 50 elements. Again, the self-adaptive capability of the method in solving problems with complicated postbuckling response has been demonstrated in this example.

Conclusions

A generalized displacement control method has been proposed for geometrically nonlinear analysis and has been proven to be very effective by several problems with multiple limit points and snap-back points. This method can be implemented easily in a general-purpose finite-element program for solving geometrically nonlinear problems.

Acknowledgments

This research was sponsored by the National Science Council of the Republic of China under Grant NSC78-0410-E002-30.

References

[1]Argyris, J. H., "Continua and Discontinua," *Proceedings of First Conference on Matrix Methods in Structural Mechanics*, Wright-Patterson Air Force Base, Ohio, 1965, pp. 11-89.

[2]Pian, T. H. H., and Tong, P., "Variational Formulation of Finite Displacement Analysis," *Proceedings of IUTAM Symposium on High Speed Computing of Elastic Structures*, edited by B. F. de Veubeke, Univ. of Liege, Liege, Belgium, 1971, pp. 43-63.

[3]Zienkiewicz, O. C., "Incremental Displacement in Non-Linear Analysis," *International Journal for Numerical Methods in Engineering*, Vol. 3, 1971, pp. 587-588.

[4]Wempner, G. A., "Discrete Approximation Related to Nonlinear Theories of Solids," *International Journal of Solids and Structures*, Vol. 7, 1971, pp. 1581–1599.

[5]Riks, E., "The Application of Newton's Methods to the Problem of Elastic Stability," *Journal of Applied Mechanics*, Vol. 39, 1972, pp. 1060–1066.

[6]Riks, E., "An Incremental Approach to the Solution of Snapping and Buckling Problems," *International Journal of Solids and Structures*, Vol. 15, 1979, pp. 529–551.

[7]Ramm, E., "Strategies for Tracing the Nonlinear Response Near Limit Point," *Nonlinear Finite Element Analysis in Structural Mechanics*, edited by W. Wunderlich, E. Stein, and K.-J. Bathe, Springer-Verlag, Berlin, 1981, pp. 63–89.

[8]Crisfield, M. A., "A Fast Incremental/Iterative Solution Procedure That Handles Snap-Through," *Computers & Structures*, Vol. 13, 1981, pp. 55–62.

[9]Crisfield, M. A., "An Arc Length Method Including Line Searches and Accelerations," *International Journal for Numerical Methods in Engineering*, Vol. 19, 1983, pp. 1269–1289.

[10]Powell, G., and Simons, J., "Improved Iteration Strategy for Nonlinear Structures," *International Journal for Numerical Methods in Engineering*, Vol. 17, 1981, pp. 1455–1467.

[11]Yang, Y. B., and McGuire, W., "A Work Control Method for Geometrically Nonlinear Analysis," *NUMETA 85—1985 International Conference on Numerical Methods in Engineering: Theory and Applications*, edited by J. Middleton and G. N. Pande, University College Swansea, Wales, UK, 1985, pp. 913–921.

[12]Batoz, J-L., and Dhatt, G. "Incremental Displacement Algorithms for Nonlinear Problems," *International Journal for Numerical Methods in Engineering*, Vol. 14, 1979, pp. 1262–1267.

[13]Tong, P., and Rossettos, J. N., *Finite Element Method—Basic Technique and Implementation*, MIT Press, Cambridge, MA, 1977.

[14]Bergan, P. G., "Solution Technique for Non-Linear Finite Element Problems," *International Journal for Numerical Methods in Engineering*, Vol. 12, 1978, pp. 1677–1696.

[15]Bergan, P. G., "Solution Algorithm for Nonlinear Structural Programs," *Numerical Methods for Non-Linear Problems*, Vol. 1, edited by C. Taylor, E. Hinton, and D.R.J. Owen, Pineridge, Swansea, Wales, UK, 1980, pp. 291–305.

[16]Pecknold, D. A., Ghaboussi, J., and Healey, T. J., "Snap-Through and Bifurcation in a Simple Structure," *Journal of Engineering Mechanics*, Vol. 111, No. 7, 1985, pp. 909–922.

[17]Harrison, H. B., "Post-Buckling Behavior of Elastic Circular Arches," *Proceedings of the Institution of Civil Engineers*, Vol. 65, Part 2, 1978, pp. 283–298.

[18]Yang, Y. B., and Chiou, H. T., "Rigid Body Motion Test for Nonlinear Analysis with Beam Elements," *Journal of Engineering Mechanics*, Vol. 113, No. 9, 1987, pp. 1404–1419.